HHS Public Access

Author manuscript

Pigment Cell Melanoma Res. Author manuscript; available in PMC 2021 July 01.

Published in final edited form as:

Pigment Cell Melanoma Res. 2020 July ; 33(4): 556–565. doi:10.1111/pcmr.12879.

Molecular characterization of *SLC24A5* variants and evaluation of Nitisinone treatment efficacy in a zebrafish model of OCA6

Sairah Yousaf[1,2], **Saumil Sethna**[1], **Muhammad A. Chaudhary**[3], **Rehan S. Shaikh**[2], **Saima Riazuddin**[1,4], **Zubair M. Ahmed**[1,4,5]

[1]Department of Otorhinolaryngology Head and Neck Surgery, School of Medicine, University of Maryland, Baltimore, MD, USA.

[2]Institute of Molecular Biology & Biotechnology, Bahauddin Zakariya University, Multan, Pakistan.

[3]Ophthalmology Department Nishtar Hospital, Multan.

[4]Department of Biochemistry and Molecular Biology, School of Medicine, University of Maryland, Baltimore, MD, USA

[5]Department of Ophthalmology and Visual Sciences, School of Medicine, University of Maryland, Baltimore, MD, USA

Abstract

Skin pigmentation is a highly heterogeneous trait with diverse consequences worldwide. *SLC24A5*, encoding a potent K^+-dependent Na^+/Ca^{2+} exchanger, is among the known color-coding genes that participate in melanogenesis by maintaining pH in melanosomes. Deficient SLC24A5 activity results in oculocutaneous albinism (OCA) type 6 in humans. In this study, by utilizing a exome sequencing (ES) approach, we identified two new variants [p. (Gly110Arg) and p. (IIe189Ilefs*1)] of *SLC24A5* cosegregating with the OCA phenotype, including nystagmus, strabismus, foveal hypoplasia, albinotic fundus and vision impairment, in three large consanguineous Pakistani families. Both of these variants failed to rescue the pigmentation in zebrafish s*lc24a5* morphants, confirming the pathogenic effects of the variants. We also phenotypically characterized a commercially available zebrafish mutant line (*slc24a5*^{ko}) that harbors a nonsense (p.Tyr208*) allele of *slc24a5*. Similar to morphants, homozygous *slc24a5*^{ko} mutants had significantly reduced melanin content and pigmentation. Next, we used these *slc24a5*^{ko} zebrafish mutants to test the efficacy of nitisinone, a compound known to increase ocular and fur pigmentation in OCA1 (*TYR*)-mutant mice. Treatment of *slc24a5*^{ko} mutant zebrafish embryos with varying doses of nitisinone did not improve melanin production and pigmentation, suggesting that treatment with nitisinone is unlikely to be therapeutic in OCA6 patients.

Correspondence: Zubair M. Ahmed, Department of Otorhinolaryngology-Head and Neck Surgery, University of Maryland School of Medicine, 670 W. Baltimore St, Room 7181, Baltimore, MD, 21021, USA. zmahmed@som.umaryland.edu.

AUTHOR CONTRIBUTIONS

Conceptualization: ZMA; Data Curation: SY, SS, MAC, ZMA; Formal Analysis: SY, SS, MAC, ZMA; Funding Acquisition: ZMA; Investigation: SY, SR, ZMA; Project Administration: ZMA; Resources: RSS, SR, ZMA; Supervision: RSS, SR, ZMA; Validation: SY, SS; Visualization: SY, SS, ZMA; Writing – Original Draft Preparation: SY, ZMA; Writing – Review and Editing: SS, RSS, SR.

CONFLICT OF INTEREST

The authors declared no conflict of interest.

Keywords

SLC24A5; NCKX5; Na^+/Ca^{2+} exchanger; OCA6; albinism; hypopigmentation

Introduction

Melanin pigmentation content determines the variability of color tones present in humans. Melanin synthesis is a highly controlled and proficient biochemical process that takes place in specific ectodermal-derived cells, known as melanocytes. Several gene products are involved in the regulation of melanin synthesis, concentration, stability and distribution. Disruption in melanogenesis either by genetic or epigenetic factors causes albinism, which is a phenotypically and genetically heterogeneous disorder. Albinism, particularly oculocutaneous albinism (OCA: loss of pigmentation from hair, iris and skin), is among the common causes of childhood vision impairment. Genetically, albinism can manifest via many inheritance patterns, although autosomal recessive albinism is the most common mode (Tomita and Suzuki, 2004). To date, pathogenic variants of six genes, *TYR*, *OCA2*, *TYRP1*, *SLC45A2*, *SLC24A5*, and *C10ORF11*, have been identified in humans suffering from nonsyndromic OCA (Gronskov et al., 2013; Gul et al., 2019; Ye et al., 2019).

Among the known OCA-associated proteins, SLC24A5 (also known as NCKX5), an eleven transmembrane domain-containing V-ATPase-dependent Na^+/Ca^{2+} exchanger pump, maintains melanosome pH by Ca^{2+} uptake (Lamason et al., 2005). SLC24A5 is a predominant Na^+/Ca^{2+} exchanger in melanocytes that possibly transports one $Ca^{2+}$and one K^+ ion to the melanosome in exchange for four cytoplasmic Na^{2+} ions (Jalloul et al., 2016). Recent studies have revealed that humans cases of OCA type 6 and zebrafish “golden” mutant phenotypes are due to pathogenic variants in SLC24A5 (Bertolotti et al., 2016; Lamason et al., 2005; Lasseaux et al., 2018). Clinical presentation of OCA6 in humans is highly variable with milder to hypopigmented skin, light/blonde brown hair and reduced to no pigmentation in the iris. Other ocular characteristics include reduced vision, nystagmus, iris transillumination and foveal hypoplasia (Lasseaux et al., 2018; Veniani et al., 2016).

Clinically, for individuals manifesting OCA, there are few supportive measures available, including using low vision aids, avoiding prolonged sun exposure, and employing the best corrected refractive error, which are certainly not preventive or sufficient. Nitisinone, an FDA-approved drug, is used to treat tyrosinemia type 1 and acts by inhibiting the enzyme 4-hydroxyphenylpyruvate dioxygenase (in the tyrosine catabolism pathway) and causes an elevated level of tyrosine in the patient’s blood plasma but has side effects (Das, 2017). Nitisinone increases plasma tyrosine and melanin production by stabilizing the mutant tyrosinase in OCA1 mutant mice (Onojafe et al., 2011). Recently, a clinical trial of nitisinone in OCA1B human subjects showed improved skin and hair pigmentation with no impact on iris melanin content (Adams et al., 2019). In this study, we document the clinical presentation, genetics and functional analysis of two novel *SLC24A5* variants segregating in three large consanguineous Pakistani families. We also characterized the pigmentation and visual phenotype of a new zebrafish model of *slc24a5*. Finally, we evaluated the efficacy and

efficiency of nitisinone in improving melanin synthesis and pigmentation in the *slc24a5*$^{ko/ko}$ zebrafish.

Materials and Methods

Family recruitment and clinical examination

The current study followed the tenets of the Declaration of Helsinki and was approved by Institutional Review Boards (IRB) at University of Maryland, USA and Bahauddin Zakariya University, Pakistan. Three Pakistani families with nonsyndromic oculocutaneous albinism were recruited to participate in this collaborative study. Written informed consent was obtained from all adult subjects and parents of minor subjects. Clinical assessments, including iris color, strabismus, photophobia, nystagmus, visual acuity and fundoscopy, were performed at Nishtar Hospital. Blood samples were collected for genomic DNA isolation after explaining the promising consequences of the study to the subjects.

Exome Sequencing (ES)

One of the affected samples from each family PKAB163 and PKAB175 was submitted to the Center for Mendelian Genomics (CMG) for ES. Yale University CMG established the protocol for ES, comprising library formation, exome capture, HiSeq next-generation sequencing and data evaluation. The affected individuals of family PKAB173 were screened for all known OCA genes by the method described previously (Jaworek et al., 2012).

Bioinformatics

To evaluate the pathogenic consequences of the identified mutations, we used four online pathogenicity prediction programs including SIFT, Polyphen2, MutationTaster, MutationAssessor and Varsome database. Phyre2 and HOPE prediction programs were used to generate wild-type and mutant protein 3D structures and explore the effects of identified mutations on SLC24A5 protein function respectively. Multiple sequence alignment of the protein was performed using Clustal omega.

Expression constructs preparation

A full-length zebrafish *slc24a5* cDNA construct was cloned in both pEGFP-C2 (Clontech, Mountain View, CA) and T7Ts (Addgene, Watertown, MA) vectors to carry out subcellular localization studies and *slc24a5* knockdown zebrafish rescue experiments. Quikchange Site Directed Mutagenesis kit (Stratagene, La Jolla, CA) was used to generate mutant constructs by employing wild-type cDNA as template.

Immunofluorescence assay

For the subcellular colocalization study, human melanocytes (C32, ATCC CRL-1585) were seeded onto coverslips and transiently transfected with Lipofectamine 2000 (Invitrogen, Carlsbad, CA). After 48 hours of transfection, cells were washed and fixed in 4% PFA for 20 min followed by subsequent permeabilization in 0.1% Triton X-100 for 15 min at room temperature (RT). Afterwards, 10% NGS (1 hour at RT) was used to block the cells. Anti-calregulin (Santa-Cruz Biotechnology, Santa Cruz, CA), Lamp1 (DSHB) and DAPI were

used to stain the endoplasmic reticulum, lysosomes and nucleus respectively. For imaging cells, a Zeiss LSMDUO confocal microscope was used.

Zebrafish *slc24a5* Morpholino (MO) knockdown and mRNA rescue

Zebrafish *slc24a5*-ATG-blocking MO (5' GCTGGAGAAACACGTCTGTCCTCAT 3') was purchased from Gene Tool, LLC (Philomath, OR). Lyophilized MO was resuspended in high-grade water (stock conc. 25 ng/nl). A standard scrambled MO was used as a negative control. Stock solution was diluted to 2.5 ng/nl to inject 5 ng/embryo. A working dilution of 0.05% phenol red was added to ensure proper microinjection in the yolk. After microinjections, embryos were kept at 28 °C in E3 embryo water. The phenotype was documented after 72 hours by making 4 different classes. For the rescue experiment, zebrafish wild-type and mutant *slc24a5* constructs were cloned in pT7Ts, mRNA was synthesized *in vitro* using the T7 mMessage mMachine kit (Ambion, Austin, TX), and 250 pg was used for microinjection.

slc24a5^{ko} phenotype characterization and electroretinography

Zebrafish larval and adult pigmentation was phenotyped by acquiring images using Infinity 3 Lumenera. For histological analyses, one-year-old adult fish (n=3 each WT and *slc24a5*$^{ko/ko}$) were sacrificed in 0.05% tricaine (3-amino benzoic acid ethyl ester) until unresponsive, and their eyes were fixed in Davidson's fixative solution overnight at 4 °C and processed for paraffin sectioning. Then, 10-μM-thick transverse sections were collected and stained with hematoxylin (Thermo Scientific, Waltham, MA) and Eosin Y (95%, Sigma, St. Louis, MO) to evaluate the overall retinal tissue morphology. Images were collected on a Nikon Eclipse TE300 microscope at 40X. Later, ImageJ was used to measure the thickness of different retinal cell layers. Thickness of each retinal layer was measured at 5 different locations and obtained readings were then used to plot the graph and one-way ANOVA (post-hoc Tukey's test) was performed to analyze the data.

Retina electrophysiology examined in seven to ten-month-old WT (n=7) and *slc24a5*$^{ko/ko}$ (n=6) zebrafish that were dark-adapted overnight. All of the following procedures were performed under dim red light. Fish were anesthetized by submersion in tricaine solution. After anesthesia, zebrafish were transferred to a wet Whatman filter paper stack and immobilized by injection of 10 μL of 25 mg/ml gallamine triethiodide (Enzo Life Sciences, East Farmingdale, NY) below the gills. Anesthesia was maintained with continuous perfusion of tricaine-containing oxygenated system water. The reference AgCl electrode was placed near the eye and the recording electrode was placed on the eye. The fish with attached electrodes was placed in a Ganzfeld chamber and presented with increasing scotopic stimuli (0.025–9.952 cd x s/m2) at 10–60 sec intervals using UTAS BigShot (LKC Technologies, Gaithersburg, MD). A minimum of 3 waveforms per intensity were averaged.

Nitisinone treatment assay

To evaluate the effect of nitisinone on *slc24a5* knock out zebrafish, Nitisinone (SML0269) was purchased from Sigma and dissolved in 2 M NaOH and $NaHCO_3$ (to neutralize the pH) to a final stock concentration of 150 mM. A dose range of 1 to 200 μm was selected to assess the zebrafish drug toxicity. The selected dose was administered by adding it to E3

medium as early as 0 hpf. We used 2 M NaOH and $NaHCO_3$ solution as a carrier. The treated embryos were kept at 28 °C and we changed the drug water after every 24 hours until 7 days. Treated embryos were imaged from day 1 to day 7 using the Infinity 3 Lumenera camera. Then, embryos were collected to perform the melanin assay.

Melanin assay

At 7 dpf, 100 larvae (of each treatment conc.) were anesthetized on ice and 300 μl of homogenization buffer (1 mM PMSF, 2 mM EGTA and 20 mM Tris-HCl, pH 7.1) was added. The larvae were kept immediately at −80 °C overnight. The following day, we used a disposable pestle to homogenize the larval whole bodies and subsequently added 100 μl of water, 100 μl of DMSO and 500 μl of 2 M NaOH to each tube. For the standard melanin curve, we used freshly prepared melanin (M2649, common cuttlefish) from Sigma dissolved in 1% hydrogen peroxide at a concentration of 1 mg/ml. The following melanin concentration gradient was used to make the standard curve: 0, 50, 100, 150, 200, 250, 200, 350 and 400 μg/ml. Standard and larval samples were boiled at 80 °C for 2 hours with subsequent centrifugation at 12000 g for 10 min at room temperature. After centrifugation, we collected the supernatant and took absorbance at 350 nm using a nanodrop 2000c spectrophotometer (Thermo Scientific). The obtained readings were then used to plot the graph and larval melanin quantification by Prism GraphPad.

Results

Identification, clinical and molecular characterization of OCA6 in Pakistani families

Through comprehensive genetic screening of 160 consanguineous families enrolled from various regions of Pakistan after institutional review board approval, we identified three large pedigrees segregating pathogenic variants of *SLC24A5* (Figure 1). To the best of our knowledge, this report is the first to describe the occurrence of OCA6 in the Pakistani population. Affected individuals of all three families had salient clinical features of nonsyndromic OCA, including yellow-brown hair, white skin, nystagmus, low visual acuity, albinotic fundus and foveal hypoplasia (Table 1). The affected individuals of family PKAB173 had black spots on their skin with sun-burned lips (Figure 1). Dilated fundus examination of family PKAB163 affected individuals (III:16 and III:17) revealed the presence of an abnormal choroidal vascular manifestation that reflects low retinal pigmented epithelium (RPE)/choroidal melanin content (Figure 2). Affected individuals (VI:1 and VI:2) of family PKAB175 also showed a prominent choroidal vascular pattern, diminished pigmentation and hypoplastic fovea (Figure 2). Both affected individuals also appeared to have an annular reflex of macula (Figure 2, arrows), suggesting some foveal development, however, no obvious foveal reflex were observed.

Exome sequencing (ES) followed by Sanger sequencing revealed a novel *SLC24A5* pathogenic missense variant [c.328G>C, p. (Gly110Arg)] segregating with the disease phenotype in the PKAB163 family (Figure 1). No other homozygous or compound heterozygous potentially pathogenic variants in other known albinism genes were observed in the exome data. All affected individuals of families PKAB173 and PKAB175 were homozygous for a novel deletion variant (c.564_568delTATAA) of *SLC24A5* (Figure 1,

Table 1). Deletion of five base pairs is predicted to cause a reading frame shift and premature truncation [p.(Ile189Ilefs*1] of the encoded protein (Figure 3A). Missense variant [p.(Gly110Arg)] of *SLC24A5* is found in ExAC and gnomAD with allele frequencies of 0.00001649 and 0.00001194, respectively. However, we did not find truncation variant [p.(Ile189Ilefs*1)] in both databases (Table 1). Additionally, we did not find these variants in 113 ethnically matched control chromosomes or in exome sequence data from 250 unrelated Pakistani individuals with non-albinism traits.

To assess the impact of identified variants on the protein structure, we performed *in silico* molecular modeling. Replacement of an evolutionary conserved glycine residue at position 110 (Figure S1) with arginine is predicted to be pathogenic by several *in silico* algorithms (Table 1). We also used the HOPE and Phyre2 prediction programs to further assess the effect of the p.(Gly110Arg) variant on the secondary structure of the encoded protein. Glycine replacement with arginine is predicted to introduce a charge that results in the repulsion of similarly charged ligands (Figure 3A); however, the hydrogen bonding pattern did not appear to be affected by this replacement. Additionally, due to the size difference between glycine and arginine, this substitution might also lead to bumps in the secondary structure. Furthermore, glycine is flexible enough to make torsion angles, and replacement of it with arginine will force the local backbone to take an incorrect conformation and begin interacting with nearby residues, which will affect the secondary structure (Figure 3A). For comparison, we also modeled two of the previously reported missense variants, p.Ala115Glu and p.Ser182Arg, that are associated with OCA6 in humans (Figure S2). Introduction of a large negatively charged glutamic acid at position 115 results in a hydrophobicity difference. Although the native alanine at position 115 is not directly involved in ligand binding, glutamic acid substitution is predicted to impact the lipid membrane interactions by altering local stability and ligand-contacts made by one of the neighboring residues (Figure S2). Similarly, p.Ser182Arg variants result in positive charge induction and size difference, which affects interaction with nearby residues with an eventual loss of lipid-membrane interactions (Figure S2). In contrast, the isoleucine at position 189 is shown to be involved in making a hydrogen bond with p.Ala184 and p.Asp192, which is predicted to be lost due to p.(Ile189Ilefs*1) variant segregation in families PKAB173 and PKAB175 (Figure 3A).

Functional analysis of SLC24A5 variants in heterologous cells and zebrafish morphants

To functionally validate the *in silico* predictions, we next investigated the impact of variants identified in this study, as well as the two previously reported missense variants (p.Ala115Glu; p.Ser182Arg), on the stability and/or targeting of SLC24A5 in human melanocyte heterologous cells. Human melanocytes were transiently transfected with GFP-tagged, full-length wild-type or mutant cDNA constructs (Figure 3B). Forty-eight hours posttransfection, cells were fixed and coimmunostained with calregulin (endoplasmic reticulum marker), Lamp1 (lysosomal-associated membrane protein 1) and DAPI (nuclei marker). Wild-type and mutation-harboring SLC24A5 was localized predominantly throughout the cytoplasm of melanocytes with some expression in the ER (Figure 3B). No apparent difference in the levels and localization of SLC24A5 mutant proteins was observed compared with wild-type SLC24A5 (Figure 3B, Table S1).

Next, for further functional evaluation of the identified variants, we developed a zebrafish morphant model of *slc24a5*. Knocking down *slc24a5* expression using morpholinos has been shown to result in loss of pigmentation in zebrafish eyes and skin (Lamason et al., 2005). Using the reported ATG-specific translation blocking morpholino (MO) injected at the 1–2 cell stage, we studied the impact on pigmentation at various developmental stages. First, a dose-escalation study using various concentrations (5.0, 5.5, 6.0, 7.0 and 7.5 ng) of MO was performed (Figure S3). MO-injection in embryos resulted in multiple development abnormalities that we classified in four groups based on the severity of the phenotype and pigmentation (Figure 4A). High dose (≥6.0 ng)-treated zebrafish also showed larger yolks, curved bodies and early larval lethality (up to 93%; Figure S3). Therefore, 5.5 ng was selected as the optimum dose for further studies based on the observed hypopigmentation phenotype with normal gross morphology of most morphants (Figure S3). During development, uniform melanin appearance in the eye and other parts of the zebrafish can be observed at approximately 30 hpf (Camp and Lardelli, 2001). We selected 72 hpf as a reference time point to characterize the pigmentation phenotype in control (scrambled MO) and *slc24a5* MO-injected embryos. As anticipated (Lamason et al., 2005), most (>90%) *slc24a5* morphants but not the control injected embryos had hypopigmentation of the iris and body (Figure 4A–B, class III).

Next, to assess the pathogenic effect of the OCA6 variants (p.Gly110Arg, p.Ile189Ilefs*1, p.Ala115Glu and p.Ser182Arg), we coinjected zebrafish embryos with either 250 pg WT or mutation-harboring *slc24a5* mRNA along with MOs and scored the pigmentation phenotype at 72 hpf (Figure 4B). Importantly, we were able to significantly (ANOVA: $p<0.005$) rescue the morphant phenotypes with coinjection of WT *slc24a5* mRNA (Figure 4B). However, rescue of the morphant phenotypes (all classes including normal) by coinjection of *slc24a5* MO and the zebrafish *slc24a5* mRNA with either c.328G>C (p.Gly110Arg) or c.564_568delATATA (p.Ile189Ilefs*1) mutations was not statistically significant compared with corresponding categories in *slc24a5* MO-alone injections, suggesting their complete loss-of-function impact (Figure 4B). However, compared to embryos injected with only *slc24a5* MO, we did observe an increase in normal-looking embryos with partial rescue of the pigmentation when *slc24a5* MO was coinjected with *slc24a5* mRNA encoding protein harboring either p.Ala115Glu or p.Ser182Arg, indicating their hypomorphic nature (Figure 4B).

Evaluation of nitisinone as a candidate drug for treatment of *SLC24A5* (*OCA6*)-associated albinism

As mentioned above, nitisinone treatment revealed increased pigmentation in OCA1 mutant mice (Onojafe et al., 2011). In this study, we sought to evaluate the efficacy and efficiency of nitisinone in restoring pigmentation in the OCA6 zebrafish model. For this study, the commercially available *slc24a5* knockout line (p.Tyr208*) was used, which we first phenotypically and functionally characterized. After confirming the genotypes, we documented the pigmentation profile of homozygous mutants along with WT controls from 48 hpf to adult stages. There was a remarkable general hypopigmentation in $slc24a5^{ko/ko}$ fish as early as 48 hpf (Figure 5A), which persisted through adulthood (Figure 5B–C). We assessed retinas of $slc24a5^{ko/ko}$ adults and found no impairment of the retinal architecture,

with the ganglion cell layer, nuclear layers, and photoreceptor layers all being observed to be intact, except for the inner plexiform layer (IPL), which was found to be significantly different (ANOVA **p<0.005, Figure 5D). To assess the functional impact of *slc24a5*$^{ko/ko}$ on vision, we performed full-field electroretinograms (ERGs) on WT and *slc24a5*$^{ko/ko}$ zebrafish at 7–10 months of age. Noninvasive *in vivo* scotopic ERGs showed no significant differences in b-wave amplitudes in the *slc24a5*$^{ko/ko}$ zebrafish compared to controls (Figure 5E), indicating intact photoreceptor response in these animals.

After phenotyping these *slc24a5* mutants, we performed a dose-escalation study using the nitisinone drug. Embryos from the *slc24a5*$^{ko/ko}$ crosses along with WT embryos were housed in water containing various nitisinone concentrations (1.0, 2.5, 5, 10, 20, 50, 100, 150 and 200 μm), and the resulting effects on pigmentation were documented at 72 hpf (Figure S4). As apparent from the representative images shown in Figure S4, higher doses (>20 μm) of nitisinone interfered with fish development. Therefore, we selected three concentrations, 2.5, 5.0 and 10 μm, for further efficacy studies (Figure 6, and Figure S5).

The *slc24a5*$^{ko/ko}$ mutant and control embryos were housed in water containing 2.5, 5.0 or 10 μm nitisinone, and imaged every day until day 7 to document the effect on the number, size and migration of melanosomes in the body. No apparent difference in the pigmentation pattern was observed in the treated *slc24a5*$^{ko/ko}$ fish compared with untreated mutants (Figure 6). On processing of the images using ImageJ and analysis of the data using a 2-tailed *t*-test, we did not observe any statistically significant difference in the number, size and distribution of melanosomes in the treated *slc24a5*$^{ko/ko}$ fish compared with untreated mutants. Furthermore, to quantify the melanin content, we performed a melanin assay using melanin from Sepia Officinalis as a standard at 7 dpf. A melanin standard curve was used to interpolate the treated fish melanin contents and one-way ANOVA (post hoc Tukey's test) was used to analyze the data. No statistically significant difference in melanin content was found in the treated *slc24a5*$^{ko/ko}$ fish for any of the nitisinone concentrations (2.5, 5 and 10 μm) compared to untreated and carrier controls (Figure S6). These data demonstrate that treatment with nitisinone does not have a major impact on melanin pigmentation, size, number and distribution of melanosomes in the *slc24a5*$^{ko/ko}$ zebrafish model of OCA6.

Discussion

SLC24A5, a potent K^+-dependent Na^+/Ca^{2+} exchanger, plays a vital role in melanogenesis by maintaining ionic homeostasis inside the melanosomes. Genetic variants significantly impact the function of SLC24A5, resulting in the OCA6 type 6 phenotype in humans and complete loss of pigmentation in zebrafish (Bertolotti et al., 2016; Ceyhan-Birsoy et al., 2019; Lamason et al., 2005; Lasseaux et al., 2018; Mondal et al., 2012; Morice-Picard et al., 2014; Veniani et al., 2016; Wei et al., 2013). Our study further expands the genetic repertoire of SLC24A5 variants responsible for OCA6 in humans, especially in the Pakistani population. Our three large consanguineous Pakistani families segregate two novel *SLC24A5* homozygous pathogenic variants (Table S2) that lead to the OCA phenotype, similar to previously reported individuals (Morice-Picard et al., 2014; Wei et al., 2013). Although both variants did not impact the expression, stability and localization of the encoded protein in heterologous cells, our humanized *slc24a5* mutant mRNAs failed to

rescue the zebrafish morphant phenotype (Figure 4B), substantiating the pathogenic impact on the protein function.

Melanocyte-secreted melanin pigment helps prevent human skin from different damage e.g., free radicals, UV radiation and reactive oxygen species. Intriguingly, single nucleotide polymorphisms (SNPs) in *SLC24A5* are also known to influence natural human skin color variations (Stokowski et al., 2007). For instance, the p.Ala111Thr SNP in SLC25A5 has been associated with light skin color in Europeans (Basu Mallick et al., 2013). Extrapolating these findings, regulation of *SLC24A5* expression through, for example, the use of small molecules or advanced genome editing tools (e.g., CRISPR)(Chiarella et al., 2019), might improve the melanin pigment and associated visual function in individuals suffering with albinism. The zebrafish is attracting attention from researchers as model organism to perform genome-editing-based interventions and small molecule-based drug screens for genes responsible for the OCA phenotype in humans. Previous studies have demonstrated that both prenatal and postnatal treatment with nitisinone elevated tyrosine levels in the *Tyr* mouse models of albinism (OCA1) (Onojafe et al., 2011). Intriguingly, a small pilot clinical study at the National Eye Institute (NEI) suggests that nitisinone treatment increases melanin production in some people with oculocutaneous albinism type 1B (OCA1B). Encouraged by these findings, we performed nitisinone treatment evaluation in an OCA6 zebrafish model. For these studies, we first established and thoroughly characterized a zebrafish model of SLC24A5, harboring an early truncating variant. Although treatment of these mutants with various concentration of nitisinone did not improve the melanin content and pigmentation in the developing embryos, our study established an animal model for preclinical evaluation of other potential therapeutic interventions (e.g., L-DOPA treatment). Furthermore, studies of these zebrafish mutants may help to elucidate the function of SLC24A5 in the multiple and complex events of melanogenesis.

Supplementary Material

Refer to Web version on PubMed Central for supplementary material.

ACKNOWLEDGMENTS

We thank the participants for their cooperation. We also thank Drs. F. Zulfiqar and M. Shahzad for technical assistance. This study was supported by National Institute of Arthritis and Musculoskeletal and Skin Diseases (NIAMS/NIH) research grant R56AR065483 to ZMA.

References

Adams DR, Menezes S, Jauregui R, Valivullah ZM, Power B, Abraham M, Jeffrey BG, Garced A, Alur RP, Cunningham D, et al. (2019). One-year pilot study on the effects of nitisinone on melanin in patients with OCA-1B. JCI Insight 4.

Basu Mallick C, Iliescu FM, Mols M, Hill S, Tamang R, Chaubey G, Goto R, Ho SY, Gallego Romero I, Crivellaro F, et al. (2013). The light skin allele of SLC24A5 in South Asians and Europeans shares identity by descent. PLoS Genet 9, e1003912. [PubMed: 24244186]

Bertolotti A, Lasseaux E, Plaisant C, Trimouille A, Morice-Picard F, Rooryck C, Lacombe D, Couppie P, and Arveiler B (2016). Identification of a homozygous mutation of SLC24A5 (OCA6) in two patients with oculocutaneous albinism from French Guiana. Pigment Cell Melanoma Res 29, 104–6. [PubMed: 26491832]

Camp E, and Lardelli M (2001). Tyrosinase gene expression in zebrafish embryos. Dev Genes Evol 211, 150–3. [PubMed: 11455427]

Ceyhan-Birsoy O, Murry JB, Machini K, Lebo MS, Yu TW, Fayer S, Genetti CA, Schwartz TS, Agrawal PB, Parad RB, et al. (2019). Interpretation of Genomic Sequencing Results in Healthy and Ill Newborns: Results from the BabySeq Project. Am J Hum Genet 104, 76–93. [PubMed: 30609409]

Chiarella AM, Butler KV, Gryder BE, Lu D, Wang TA, Yu X, Pomella S, Khan J, Jin J, and Hathaway NA (2019). Dose-dependent activation of gene expression is achieved using CRISPR and small molecules that recruit endogenous chromatin machinery. Nat Biotechnol.

Das AM (2017). Clinical utility of nitisinone for the treatment of hereditary tyrosinemia type-1 (HT-1). Appl Clin Genet 10, 43–48. [PubMed: 28769581]

Gronskov K, Dooley CM, Ostergaard E, Kelsh RN, Hansen L, Levesque MP, Vilhelmsen K, Mollgard K, Stemple DL, and Rosenberg T (2013). Mutations in c10orf11, a melanocyte-differentiation gene, cause autosomal-recessive albinism. Am J Hum Genet 92, 415–21. [PubMed: 23395477]

Gul H, Shah AH, Harripaul R, Mikhailov A, Prajapati K, Khan E, Ullah F, Zubair M, Ali MZ, Shah AH, et al. (2019). Genetic studies of multiple consanguineous Pakistani families segregating oculocutaneous albinism identified novel and reported mutations. Ann Hum Genet.

Jalloul AH, Rogasevskaia TP, Szerencsei RT, and Schnetkamp PP (2016). A Functional Study of Mutations in K+-dependent Na+-Ca2+ Exchangers Associated with Amelogenesis Imperfecta and Non-syndromic Oculocutaneous Albinism. J Biol Chem 291, 13113–23. [PubMed: 27129268]

Jaworek TJ, Kausar T, Bell SM, Tariq N, Maqsood MI, Sohail A, Ali M, Iqbal F, Rasool S, Riazuddin S, et al. (2012). Molecular genetic studies and delineation of the oculocutaneous albinism phenotype in the Pakistani population. Orphanet J Rare Dis 7, 44. [PubMed: 22734612]

Lamason RL, Mohideen MA, Mest JR, Wong AC, Norton HL, Aros MC, Jurynec MJ, Mao X, Humphreville VR, Humbert JE, et al. (2005). SLC24A5, a putative cation exchanger, affects pigmentation in zebrafish and humans. Science 310, 1782–6. [PubMed: 16357253]

Lasseaux E, Plaisant C, Michaud V, Pennamen P, Trimouille A, Gaston L, Monferme S, Lacombe D, Rooryck C, Morice-Picard F, et al. (2018). Molecular characterization of a series of 990 index patients with albinism. Pigment Cell Melanoma Res 31, 466–474. [PubMed: 29345414]

Mondal M, Sengupta M, Samanta S, Sil A, and Ray K (2012). Molecular basis of albinism in India: evaluation of seven potential candidate genes and some new findings. Gene 511, 470–4. [PubMed: 23010199]

Morice-Picard F, Lasseaux E, Francois S, Simon D, Rooryck C, Bieth E, Colin E, Bonneau D, Journel H, Walraedt S, et al. (2014). SLC24A5 mutations are associated with non-syndromic oculocutaneous albinism. J Invest Dermatol 134, 568–571. [PubMed: 23985994]

Onojafe IF, Adams DR, Simeonov DR, Zhang J, Chan CC, Bernardini IM, Sergeev YV, Dolinska MB, Alur RP, Brilliant MH, et al. (2011). Nitisinone improves eye and skin pigmentation defects in a mouse model of oculocutaneous albinism. J Clin Invest 121, 3914–23. [PubMed: 21968110]

Stokowski RP, Pant PV, Dadd T, Fereday A, Hinds DA, Jarman C, Filsell W, Ginger RS, Green MR, Van Der Ouderaa FJ, et al. (2007). A genomewide association study of skin pigmentation in a South Asian population. Am J Hum Genet 81, 1119–32. [PubMed: 17999355]

Tomita Y, and Suzuki T (2004). Genetics of pigmentary disorders. Am J Med Genet C Semin Med Genet 131C, 75–81. [PubMed: 15452859]

Veniani E, Mauri L, Manfredini E, Gesu GP, Patrosso MC, Zelante L, D'agruma L, Del Longo A, Mazza M, Piozzi E, et al. (2016). Detection of the first OCA6 Italian patient in a large cohort of albino subjects. J Dermatol Sci 81, 208–9. [PubMed: 26686029]

Wei AH, Zang DJ, Zhang Z, Liu XZ, He X, Yang L, Wang Y, Zhou ZY, Zhang MR, Dai LL, et al. (2013). Exome sequencing identifies SLC24A5 as a candidate gene for nonsyndromic oculocutaneous albinism. J Invest Dermatol 133, 1834–40. [PubMed: 23364476]

Ye H, Lan X, Qiao T, Xu W, Tang X, Yang Y, and Zhang H (2019). [Mutation analysis of two pedigrees with suspected oculocutaneous albinism]. Zhonghua Yi Xue Yi Chuan Xue Za Zhi 36, 212–216. [PubMed: 30835348]

Significance

Here, we report two novel variants of *SLC24A5* segregating with oculocutaneous albinism (OCA6) in three Pakistani families. Both of these variants failed to rescue the pigmentation in zebrafish s*lc24a5* morphants, confirming the pathogenic effects of the variants. We also characterized the pigmentation pattern, retinal structure and visual function of zebrafish mutant strain that harbors a nonsense variant of *slc24a5*. Finally, we determine if nitisinone can improve pigmentation pattern in this *slc24a5*^{ko} zebrafish. Treatment with various concentrations of nitisinone did not improve melanin content, which indicates that as such treatment of OCA6 patients with nitisinone is unlikely to be therapeutic.

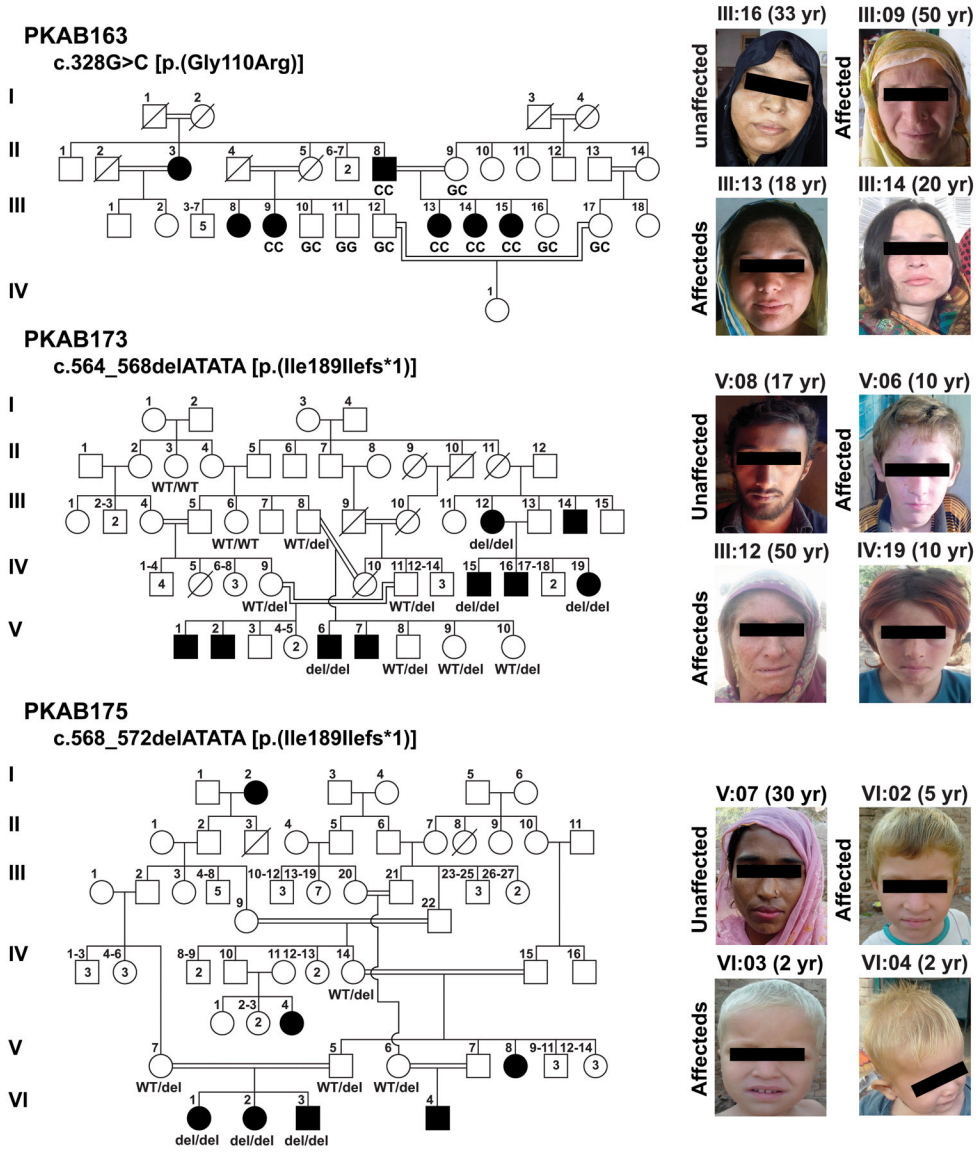

Figure 1: Variants of SLC24A5 segregate with OCA phenotype in three Pakistani families.

Pedigrees of three large consanguineous Pakistani families segregating with the OCA6 phenotype. *SLC24A5* identified variants are listed below each family ID. Empty and filled symbols represent the unaffected and affected individuals, respectively. A double line uniting two individuals represents consanguineous marriage. Below the symbols are the genotypes for the mutated alleles (WT: wild-type and del: deletion). Photographs of the individuals segregating with *SLC24A5* variants are shown in the second panel. Individual IV:19 of family PKAB173 has inbòrn light/blonde brown hair that she changed by using hair dye. Landmarks: yr, year.

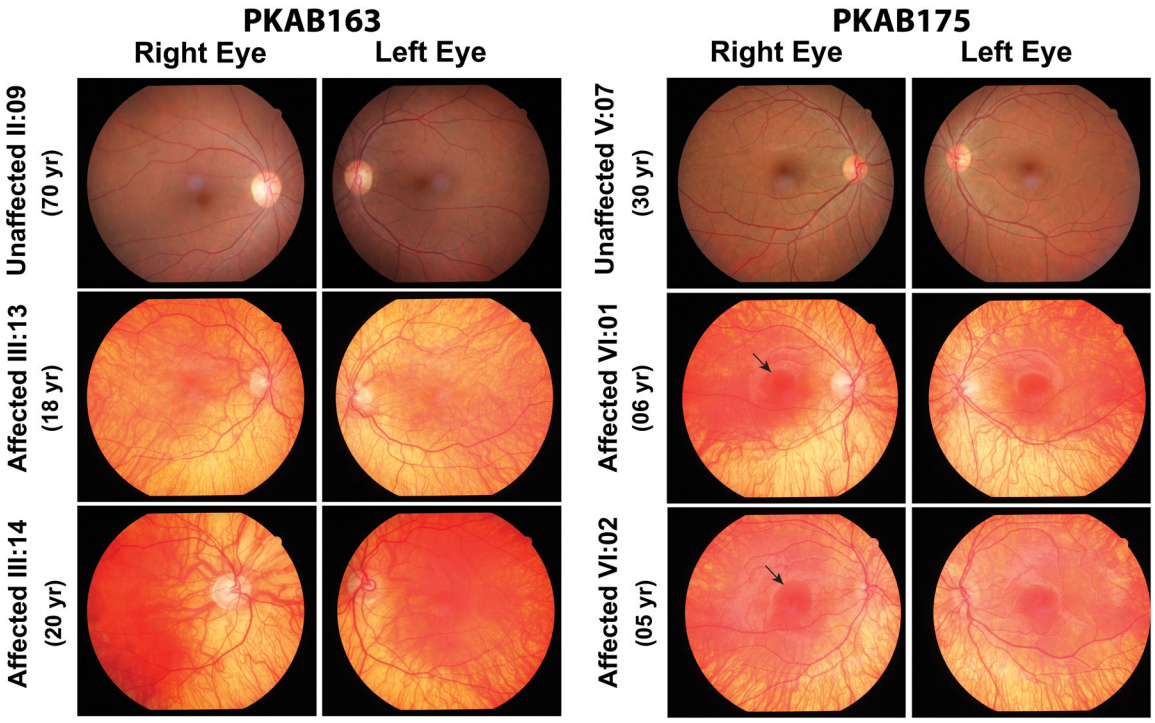

Figure 2: Fundus appearance in OCA6 affected Pakistani families.

There is reduced pigmentation in the retina of affected III: 13 of family PKAB163, which is slightly red in color compared to unaffected II: 09. However, affected individual III: 14 has severe loss of retinal pigmentation with clearly visible blood vessels, representing OCA-based fundoscopy. Similarly, the ocular manifestations of affected individuals of family PKAB175 represent an obvious choroidal vascular pattern with the entire retina having a deep red color because of a lack of melanin pigment. Arrows indicate an annular reflex of macula in both affected individuals of family PKAB175.

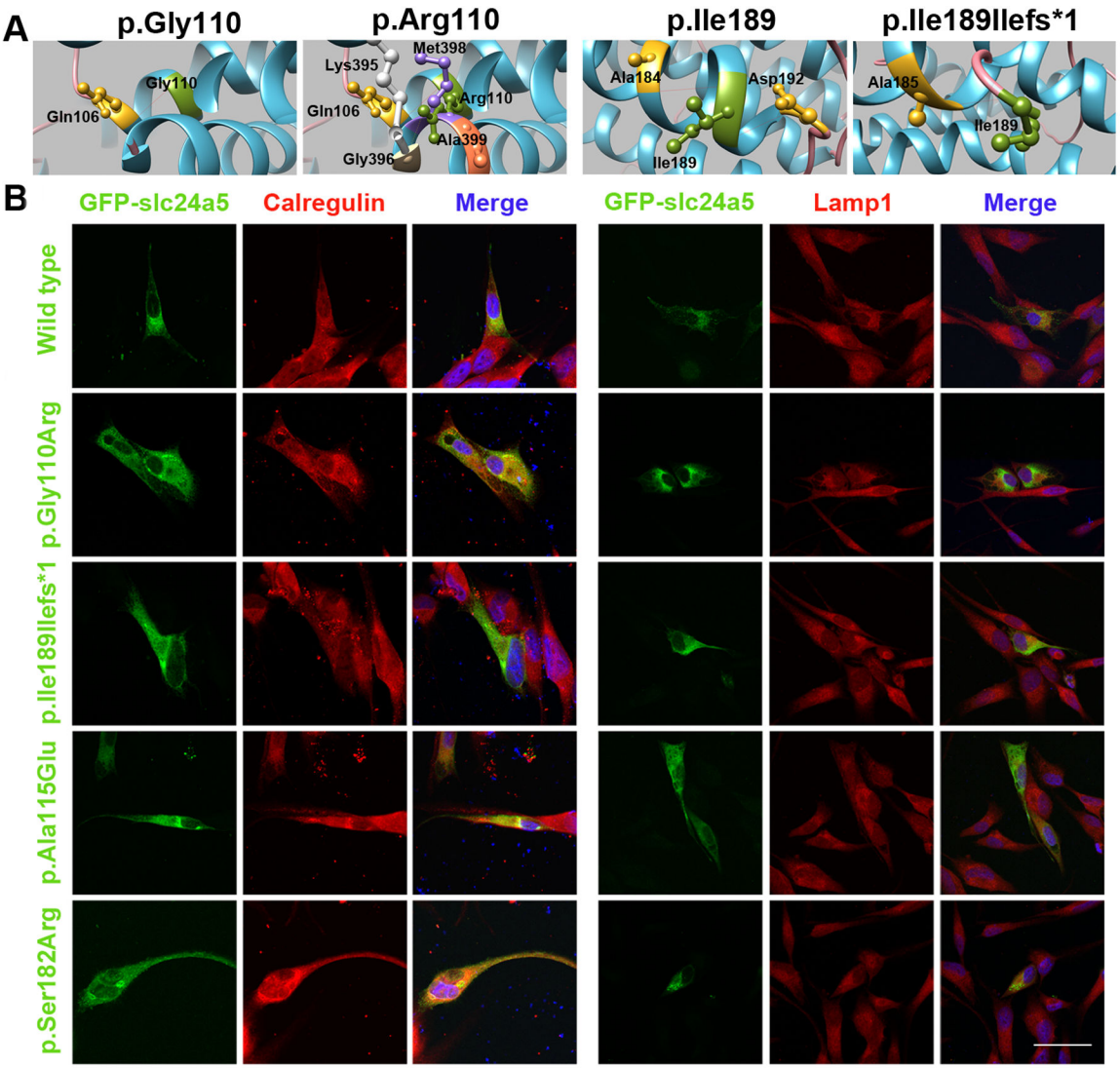

Figure 3: Functional evaluation of SLC24A5 variants.

(**a**) Comparison of SLC24A5 WT and mutant protein secondary structure. Helix and coils are shown in blue and pink colors respectively. Residues of interest are shown in olive green color. Amino acids involved in hydrogen bonding with the residue of interest are shown in goldenrod. Hydrogen bonds are shown by red lines. Interaction with nearby residues is shown by yellow dotted lines and residues in different colors. (**b**) Subcellular expression and colocalization of eGFP-tagged *slc24a5* WT and mutant constructs transiently transfected in melanocytes. No apparent difference was observed in expression of SLC25A5 harboring various mutant alleles compared to WT protein. Red represents calregulin and Lamp1, and blue represents DAPI used for staining nuclei. Scale bar: 40 μm.

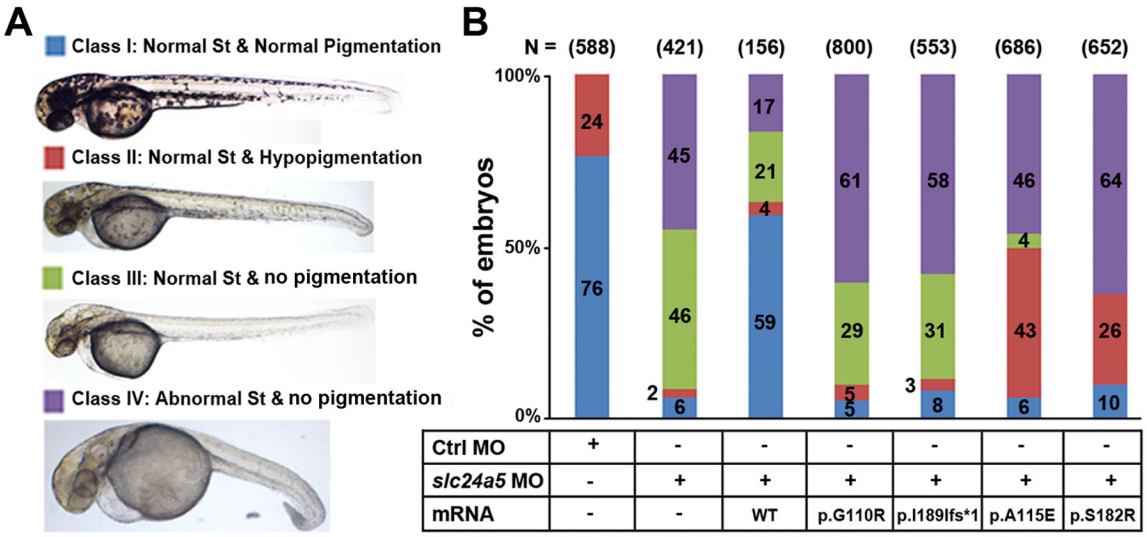

Figure 4: Functional evaluation of SLC24A5 variants in zebrafish morphants.

(**a**) Repression of *slc24a5* produces hypopigmentation and developmental defects in zebrafish embryos, which were classified into four categories. (**b**) Proportions of normal embryos are significantly rescued in embryos coinjected with WT *slc24a5* mRNA compared to mRNAs harboring OCA6 alleles.

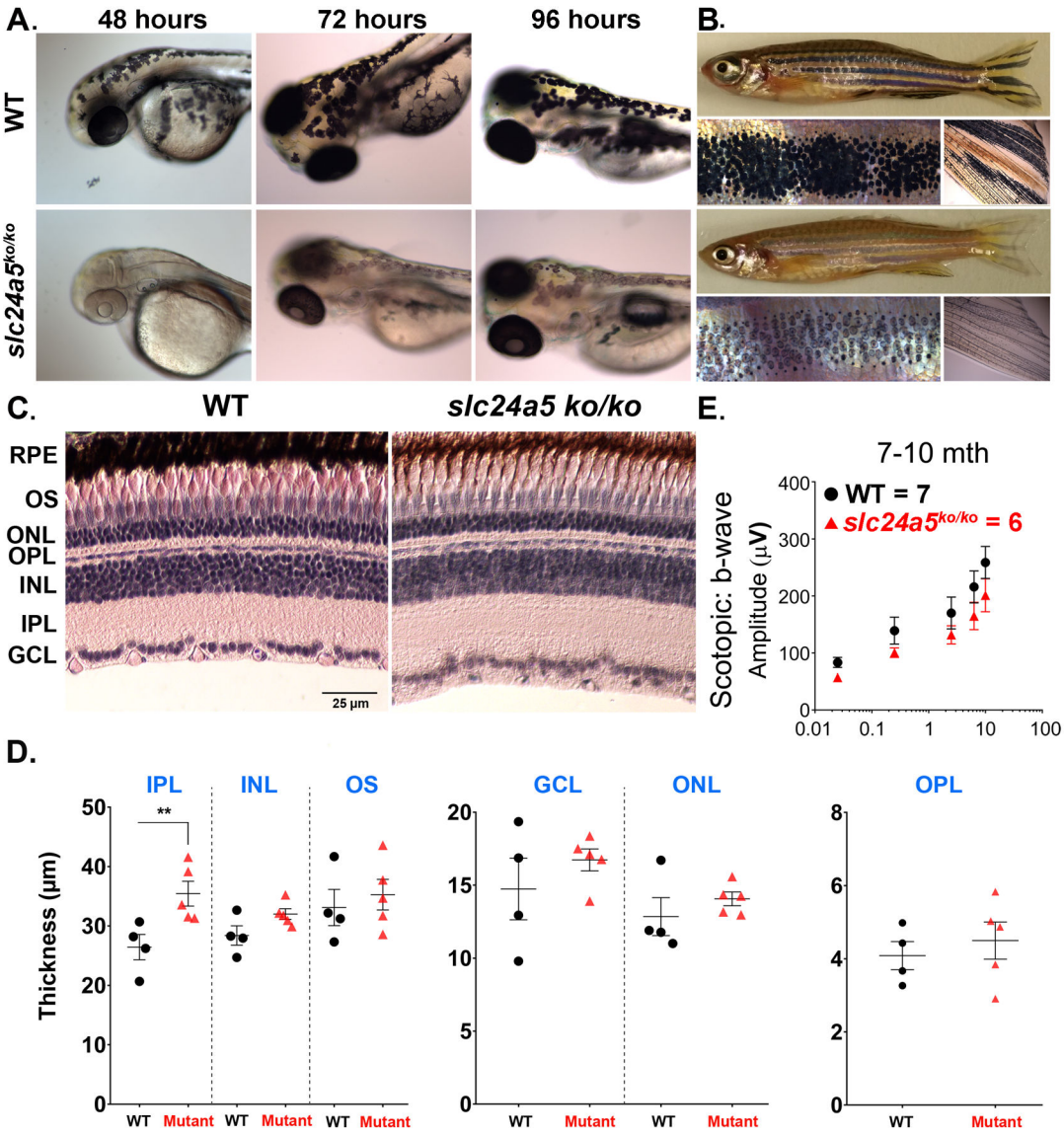

Figure 5: Characterization of pigmentary and visual function in the zebrafish *slc24a5*^{ko} model.

(**a**) Representative bright-field images of zebrafish showing hypopigmentation of RPE and skin melanocytes in *slc24a5*^{ko} at 48–96 hpf. (**b**) Bright-field images of adult *slc24a5*^{ko} fish showing low pigmented melanophores versus WT. (**c**) Zebrafish retina histology demonstrating less pigmented retina in *slc24a5*^{ko} compared to WT. (**d**) Graphical representation of retina layer thickness. There is no significant difference found in the overall retinal thickness of mutants, but the IPL is significantly larger compared to WT (Anova; **p<0.005). (**e**) Quantification of scotopic b-wave amplitudes in response to light stimulation from *slc24a5*$^{+/+}$(n = 7) and *slc24a5*$^{ko/ko}$ (n = 6) zebrafish at 7–10 months of age.

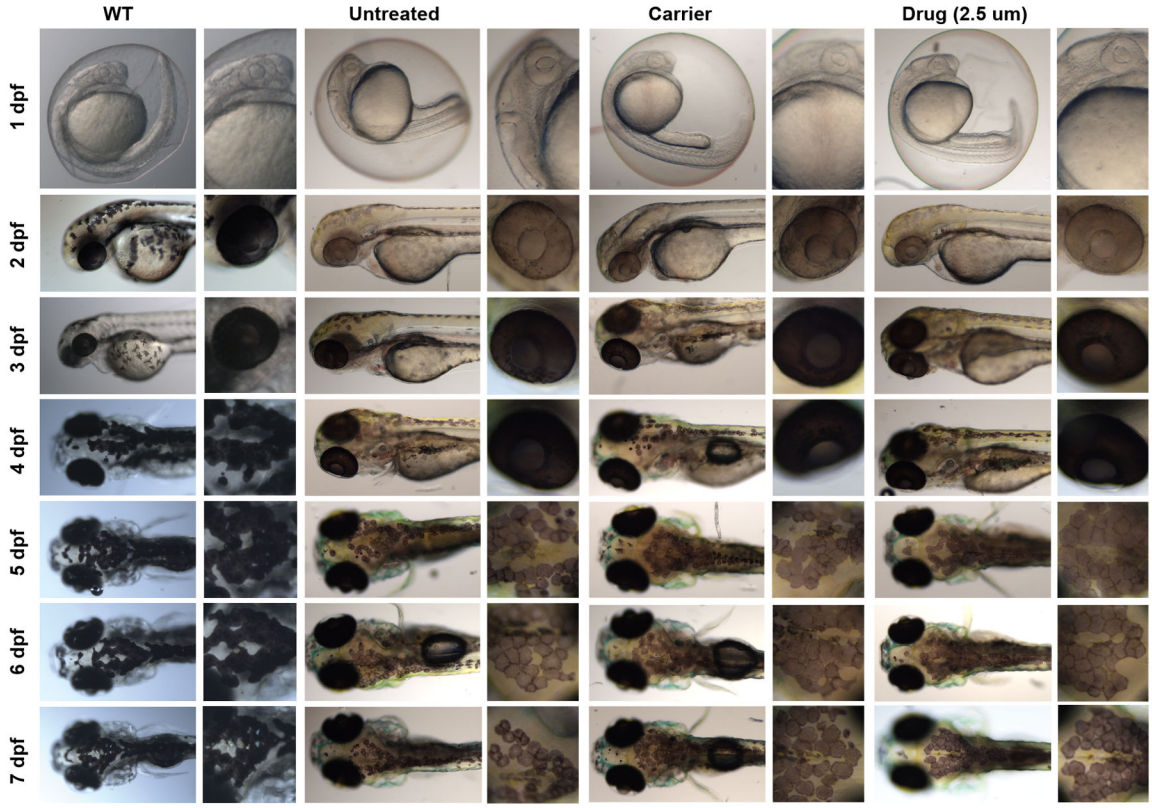

Figure 6: Representative images of *slc24a5*^{ko} larvae treated with nitisinone drug concentration of 2.5 μm.

Dorsal head images of both WT and *slc24a5*^{ko} mutant fish treated with drug carrier (as control) and nitisinone for 7 days and imaged. No apparent increase in the pigmentation profile of both treated and untreated fish was observed.

Table 1:

Clinical findings of OCA6 in Pakistani families

Family		**PKAB163**			**PKAB173**			**PKAB175**		
SLC24A5 variant		c.328G>C [p.(Gly110Arg)]			c.564_568delTATAA [p.(Ile189Ilefs*1)]			c.564_568delTATAA [p.(Ile189Ilefs*1)]		
ExAC		0.00001649			0			0		
gnomAD		0.00001194			0			0		
SIFT		Damaging			Damaging			Damaging		
PolyPhen2		Probably damaging			-			-		
MutationTaster		Disease causing			Disease causing			Disease causing		
MutationAssessor		High (FI score 3.675)			-			-		
FATHMM-MKL		Damaging			-			-		
MetaSVM		Damaging			-			-		
MetalR		Damaging			-			-		
Subject		**II:09**	**III:13**	**III:14**	**III:08**	**III:12**	**V:06**	**V:07**	**VI:01**	**VI:02**
Sex		F	F	F	M	F	M	F	F	F
Age (yrs)		70	18	20	55	50	10	30	6	5
Ethnicity		Malik			Mughal			Malan Haans		
Status		Normal	Affected	Affected	Normal	Affected	Affected	Normal	Affected	Affected
Hair color		Black	Light brown	Light brown	Black	Yellow brown	Yellow brown	Black	Yellow	Yellow
Skin tone		Wheat	White	White	Wheat	White	White	Wheat	White	White
Iris color		Brown	Hazel brown	Hazel brown	Brown	Hazel brown	Hazel brown	Brown	Brown	Brown
Visual acuity	Right	6/6	6/12	6/24	NT	NT	NT	6/6	6/60	6/12
	Left	6/12	6/12	6/18	NT	NT	NT	6/6	6/60	6/12
Refractive error		Myopic & hyperopic astigmatic	Emmetropic	Myopic & Hyperopic astigmatic	NT	NT	NT	Emmetropic	Hyperopic	Hyperopic
Fundus		Normal	Albinotic	Albinotic	NT	NT	NT	Normal	Albinotic	Albinotic
Foveal hypoplasia		No	Yes	Yes	NT	NT	NT	No	Yes	Yes
Photophobia		No	No	No	NT	NT	NT	No	No	No
Nystagmus		No	Yes	Yes	No	NT	NT	No	No	No

NT, Not Tested